

# The pro-apoptotic activity of *Drosophila* Rbf1 involves dE2F2-dependent downregulation of *diap1* and *buffy* mRNA

A Clavier<sup>1</sup>, A Baillet<sup>1</sup>, A Rincheval-Arnold<sup>1</sup>, A Coléno-Costes<sup>2,3,4</sup>, C Lasbleiz<sup>1,5</sup>, B Mignotte<sup>1</sup> and I Guénaï<sup>\*1</sup>

The retinoblastoma gene, *rb*, ensures at least its tumor suppressor function by inhibiting cell proliferation. Its role in apoptosis is more complex and less described than its role in cell cycle regulation. Rbf1, the *Drosophila* homolog of Rb, has been found to be pro-apoptotic in proliferative tissue. However, the way it induces apoptosis at the molecular level is still unknown. To decipher this mechanism, we induced *rbf1* expression in wing proliferative tissue. We found that Rbf1-induced apoptosis depends on dE2F2/dDP heterodimer, whereas dE2F1 transcriptional activity is not required. Furthermore, we highlight that Rbf1 and dE2F2 downregulate two major anti-apoptotic genes in *Drosophila*: *buffy*, an anti-apoptotic member of Bcl-2 family and *diap1*, a gene encoding a caspase inhibitor. On the one hand, Rbf1/dE2F2 repress *buffy* at the transcriptional level, which contributes to cell death. On the other hand, Rbf1 and dE2F2 upregulate *how* expression. How is a RNA binding protein involved in *diap1* mRNA degradation. By this way, Rbf1 downregulates *diap1* at a post-transcriptional level. Moreover, we show that the dREAM complex has a part in these transcriptional regulations. Taken together, these data show that Rbf1, in cooperation with dE2F2 and some members of the dREAM complex, can downregulate the anti-apoptotic genes *buffy* and *diap1*, and thus promote cell death in a proliferative tissue.

*Cell Death and Disease* (2014) 5, e1405; doi:10.1038/cddis.2014.372; published online 4 September 2014

The retinoblastoma gene (*rb*) is the first tumor suppressor identified in human cells. Its product, pRb, inhibits cell proliferation by controlling the G1/S transition.<sup>1</sup> The best characterized partners of pRB in cell cycle regulation belong to the E2F family of transcription factors.<sup>2</sup> In contrast to its tumor suppressor role, pRb is surprisingly often described as an anti-apoptotic protein.<sup>3–10</sup> However, a growing number of studies show a pro-apoptotic role for pRb.<sup>11–14</sup> *Drosophila*, which presents a lesser genetic complexity than mammals, offers the possibility to decipher the roles of Rb and E2F family proteins in apoptosis *in vivo*. Indeed, the *Drosophila* genome contains two *E2F* genes<sup>15–17</sup> (*de2f1* and *de2f2*), one *DP* gene<sup>15</sup> (*dDp*) that encodes an E2F cofactor and two *Rb* genes<sup>18,19</sup> (*rbf1* and *rbf2*). dE2F1 acts mostly as a transcriptional activator,<sup>20</sup> whereas dE2F2 represses transcription.<sup>21</sup> As pRb protein in mammals, Rbf1 can bind both activator and repressor E2F members.<sup>21</sup> Furthermore, it fulfills the same function as pRb in the cell cycle. Rbf1 is thus considered as a pRb homolog. *rbf1* loss-of-function is lethal at early larval stage<sup>20,22</sup> that attests its essential role. Homozygous *rbf1*-mutant embryos have many apoptotic cells<sup>22</sup> and it is admitted that Rbf1 protects cells by inhibiting the transcriptional activity of dE2F1 that is considered as a pro-apoptotic factor. Indeed,

*de2f1* and *dDp* co-expression induces apoptosis in the eye imaginal discs<sup>23</sup> and the pro-apoptotic genes *reaper* and *dark* are dE2F1-transcriptional targets.<sup>24,25</sup> In contrast to these data, we have previously shown that *rbf1* can also have a pro-apoptotic function. Indeed, *rbf1* overexpression in proliferating cells of wing imaginal discs leads to apoptosis and loss of tissue in adult wings.<sup>26</sup> This cell death is caspase dependent and can be inhibited by *de2f1* expression. However, the precise mechanism underlying *rbf1*-induced apoptosis is still unknown. Rbf1 being mainly described as a transcriptional regulator, one may wonder whether this activity is involved in its pro-apoptotic effect. Recent reports have clarified the role of Rbf1 in transcription. Rbf1 binding to chromatin requires dE2F/dDP complexes.<sup>27</sup> This binding is mainly observed near transcription start sites (TSS). When associated with dE2F2, Rbf1 belongs to a transcription regulator complex named dREAM<sup>28–30</sup> (*drosophila* RBF, E2F and Myb-interacting proteins). This complex maintains the transcriptional repression of certain E2F target genes in the proliferating tissues by at least two distinct mechanisms: histone deacetylation of nucleosomes near TSSs and dimethylation of histone H3 Lys27 at nucleosomes located downstream of TSSs.<sup>31</sup> Although the first reports described the dREAM complex as

<sup>1</sup>Laboratoire de Génétique et Biologie Cellulaire, EA4589, Université de Versailles Saint-Quentin-en-Yvelines, Ecole Pratique des Hautes Etudes, 2 avenue de la Source de la Bièvre, Montigny-le-Bretonneux, France; <sup>2</sup>Laboratoire de Biologie du Développement—Institut de Biologie Paris Seine, Sorbonne Universités, UPMC Univ Paris 06, UMR7622, Paris, France and <sup>3</sup>CNRS, UMR7622, Laboratoire de Biologie du Développement—Institut de Biologie Paris Seine, Paris, France

\*Corresponding author: I Guénaï, Laboratoire de Génétique et Biologie Cellulaire, EA4589, Université de Versailles Saint-Quentin-en-Yvelines, Ecole Pratique des Hautes Etudes, 2 avenue de la Source de la Bièvre 78180 Montigny-le-Bretonneux, France. Tel: +33 0 1 70 42 94 36; Fax: +33 0 1 70 42 95 03; E-mail: isabelle.guenai@uvsq.fr

<sup>4</sup>Present address: IGH—CNRS, 141 rue de la Cardonille, 34396 Montpellier, France.

<sup>5</sup>Present address: UMR Inserm U710-UM2-EPHE, Université Montpellier 2, place Eugene Bataillon-CC105, 34095 Montpellier, France.

**Abbreviations:** ChIP, chromatin immunoprecipitation; dIAP1, *Drosophila* inhibitor of apoptosis; dREAM, *drosophila* RBF, E2F and Myb-interacting proteins; en, engrailed; how, held out wings; *rb*, retinoblastoma gene; TSS, transcription start sites; vg, vestigial

Received 07.3.14; revised 23.7.14; accepted 28.7.14; Edited by E Baehrecke

an exclusive transcriptional repressor, the recent ones showed that this complex is also required to maintain the expression of some genes, highlighting that it can also participate in transcriptional activation.<sup>32</sup> Several screens have identified Rbf1 target genes.<sup>27,32,33</sup> However, how the regulation of these genes is related to the different functions of Rbf1 remains to be explained. Notably, the targets of Rbf1 in apoptosis are not known.

Here we show that Rbf1-induced apoptosis results from transcriptional regulation of at least two genes by Rbf1 and dE2F2. First, Rbf1 and dE2F2 repress the expression of *buffy*, the anti-apoptotic member of the Bcl-2 family in *Drosophila*. Second, Rbf1 and dE2F2 activate the expression of *how* (held out wings), which encodes an RNA-binding protein that destabilizes *diap1* (*Drosophila* inhibitor of apoptosis).

## Result

### dE2F2 and dDP cooperate with Rbf1 to induce apoptosis.

As previously described, overexpression of *rbf1* in the dorsal region of wing imaginal discs using the UAS-Gal4 system with the 'vestigial' (vg) Gal4 driver induced notches along the wing margin. The number of notches correlated with the

amount of apoptosis in wing imaginal discs of third instar larvae.<sup>26</sup> To determine the relative importance of the two dE2F factors in Rbf1-induced apoptosis, we performed genetic interaction tests. For each gene studied, we verified that the alteration of this gene expression level by itself (overexpression, RNAi or mutant) did not induce any wing phenotype, nor apoptosis at larval stage. Wing phenotypes were classified into four categories according to the number of notches: wild type (no notch), weak, intermediate and strong (Figure 1a). Notches were counted in the wings of flies overexpressing *rbf1* in a heterozygous *dE2F2*-mutant background (*vg-Gal4>UAS-Rbf1; dE2F2<sup>76Q1</sup>/+*) and in flies simultaneously overexpressing *rbf1* and *de2f2* (*vg-Gal4>UAS-rbf1; UAS-dE2F2*) (Figure 1b). When *rbf1* was overexpressed in *dE2F2<sup>76Q1</sup>* heterozygous context, a significant shift of the distribution toward weaker phenotypes was observed as compared with overexpression of *rbf1* alone (Figure 1b). On the contrary, when *rbf1* and *dE2F2* were co-overexpressed, the distribution significantly shifted toward stronger phenotypes. Thus, these results show that dE2F2 is necessary for Rbf1-induced notched wing phenotype. Previous data have shown that *de2f1* heterozygous loss-of-function mutant context enhances *rbf1*-induced

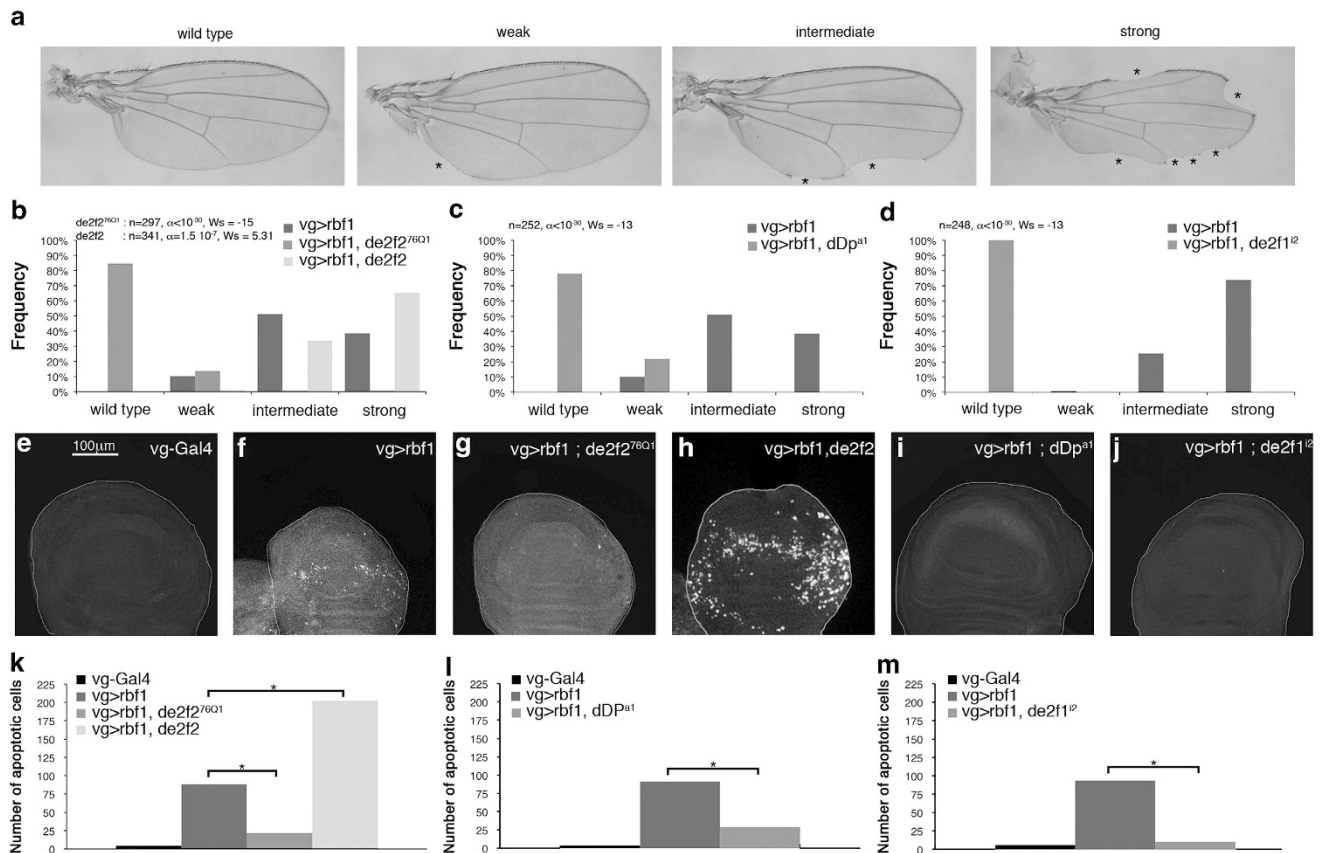


**Figure 1** Rbf1-induced apoptosis involves dE2F2 and dDP. (a) Wing phenotypes were grouped in four categories (wild type, weak, intermediate and strong) according to the number of notches observed on the wing margin (asterisks). (b–d) Distribution of notch wing phenotypes in *vg-Gal4>UAS-rbf1*, *vg-Gal4>UAS-rbf1; de2f2<sup>76Q1</sup>* and *vg-Gal4>UAS-rbf1, UAS-de2f2* (b), in *vg-Gal4>UAS-rbf1* and *vg-Gal4>UAS-rbf1; dDP<sup>a1</sup>* (c), and in *vg-Gal4>UAS-rbf1* and *vg-Gal4>UAS-rbf1; de2f1<sup>i2</sup>* (d). Statistical analysis was performed using Wilcoxon tests. Each experiment was independently performed three times; as the results were similar, only one experiment is presented here. (e–j) Apoptotic cells were visualized by TUNEL staining (white dots) of wing imaginal discs of the genotype indicated at the top of the image. All the pictures are at the same scale, scale bar: 100  $\mu$ m. (k–m) Quantification of TUNEL-positive cells in the wing pouch. Asterisks indicate a statistically significant difference between two genotypes (Student's *t*-test,  $P < 0.05$ )

notched wing phenotype, showing that *de2f1* antagonizes *rbf1*-induced phenotypes.<sup>26</sup> These results suggest that dE2F1 and dE2F2 have antagonistic roles in *rbf1*-induced notched wing phenotype. dDP is the cofactor shared by dE2F1 and dE2F2. In the absence of dDP, both dE2F1 and dE2F2 transcriptional activity is abolished.<sup>34</sup> In *dDP<sup>a1</sup>* heterozygote context, the *rbf1*-induced notched wing phenotypes significantly shifted toward weaker phenotypes (Figure 1c) as observed in dE2F2-mutant context. This result indicates that the reduction of the net transcriptional activity of dE2F factors due to *dDP*-mutant context rescues *rbf1*-induced loss of tissue. Thus, dE2F's net transcriptional activity promotes *rbf1*-induced notched wing phenotype.

We used *de2f1<sup>12</sup>* mutant to determine whether dE2F1 inhibitory role in *rbf1*-induced loss of tissue involved its transactivation domain. This dE2F1 mutant lacks both the transactivation domain and its ability to bind Rbf1.<sup>20</sup> However, it retains the DNA binding domain. By this way, it is able to bind dE2F consensus site and could exclude some complexes, such as dE2F2/Rbf1, from these genomic sites.<sup>35</sup> When *rbf1* was overexpressed in a *de2f1<sup>12</sup>* heterozygous context, the distribution of the phenotypes shifted toward weaker phenotypes as compared with the overexpression of *rbf1* alone (Figure 1d). Thus, dE2F1<sup>12</sup> suppresses *rbf1*-induced loss of tissue and the transcriptional activation mediated by dE2F1 does not seem to be required to inhibit *rbf1*-induced loss of tissue.

To verify that the variation of the phenotypic distribution between these different genetic contexts correspond to a variation of the amount of apoptosis in larvae, we performed TUNEL staining of third instar larval wing imaginal discs. Few apoptotic cells were detected in *vg-Gal4/+* control (Figure 1e). On the contrary, many cells were TUNEL labeled in *vg-Gal4/+; UAS-rbf1/+* wing discs (Figure 1f). When *rbf1* was overexpressed in a *de2f2<sup>76Q1</sup>*, *dDP<sup>a1</sup>* or *de2f1<sup>12</sup>* context (Figures 1g–j), we observed a significant decrease of TUNEL-labeled cells as compared with the overexpression of *rbf1* alone (Figures 1k–m). On the contrary, when *rbf1* and *de2f2* were co-overexpressed, the number of apoptotic cells was significantly increased (Figures 1h and k).

These data show that dE2F1 might inhibit Rbf1-induced apoptosis independently of its transactivation activity, whereas dE2F2 and dDP cooperate with Rbf1 to induce apoptosis in the wing imaginal disc, a proliferating tissue.

**Rbf1 and dE2F2 induce a reduction of *buffy* and *diap1* mRNA levels.** dE2F2 is a well-known transcriptional repressor. To explain its role in *rbf1*-induced apoptosis, we hypothesized that an Rbf1/dE2F2 complex could repress anti-apoptotic genes, leading to cell death. We focused on the two best-described anti-apoptotic factors in *Drosophila*, *diap1* and *buffy*, which encode a caspase inhibitor and a member of the Bcl-2 family, respectively. When *rbf1* was overexpressed under *vg* control, *buffy* mRNA were significantly decreased as compared with the control *vg-Gal4/+* (Figure 2a). In contrast, when *rbf1* was inactivated by RNAi (*vg-Gal4>UAS-RNAi-rbf1*), *buffy* mRNA was significantly increased as compared with the control (Figure 2b). The same result was obtained in *dDP* heterozygous loss-of-function context (data not shown). In *dE2F2<sup>76Q1</sup>* heterozygous larvae, the amount of *buffy* mRNA was similar to the one

of the control *vg-Gal4/+*. When *rbf1* was overexpressed in a *dE2F2<sup>76Q1</sup>* heterozygous context, the amount of *buffy* mRNA was similar to the one of the *vg-Gal4/+* control (Figure 2a), indicating that dE2F2 is necessary for *rbf1*-induced *buffy* mRNA decrease. These data suggest that Rbf1 represses *buffy* in wing imaginal discs in a *de2f2*-dependent manner. Similarly, *rbf1* overexpression induced a decrease of *diap1* mRNA level dependent of dE2F2 (Figure 2c). We did not observe any modification of *diap1* mRNA levels when *rbf1* was inactivated by RNAi (data not shown).

To verify whether the amount of *buffy* and *diap1* mRNA correlated with *rbf1*-induced apoptosis, we performed genetic interaction tests. When *rbf1* was overexpressed in a *buffy<sup>137</sup>* heterozygous context, distribution of the wing phenotypes shifted toward stronger phenotypes as compared with the overexpression of *rbf1* alone (Figure 2d). On the contrary, when *rbf1* and *buffy* were co-overexpressed, distribution of the wing phenotypes shifted toward weaker phenotypes. The variation of the phenotypic distribution between these different genetic contexts correlated with a variation of the amount of apoptosis in wing imaginal discs (Figure 2f). These results suggest that the decrease of *buffy* mRNA is a part of the cell death mechanism induced by Rbf1.

When *rbf1* was overexpressed and *diap1* was simultaneously inactivated by RNAi, we observed an increase of notches in the wings (Figure 2e) as well as an increase in the amount of apoptosis in wing imaginal discs (Figure 2g) as compared with the overexpression of *rbf1* alone. On the contrary, we detected a phenotypic rescue when *rbf1* and *diap1* were co-overexpressed. This suggests that *diap1* mRNA level reduction contributes to Rbf1-induced apoptosis.

**Rbf1 and dE2F2 increase *how* mRNA leading to *diap1* mRNA destabilization.** Our data suggest that Rbf1 and dE2F2 could directly repress the transcription of *diap1* and *buffy*. A putative E2F binding site is present in *buffy* 5'UTR but absent in *diap1* (data not shown). To confirm that *diap1* mRNA reduction was due to transcriptional regulation, we used a *diap1-LacZ* reporter transgene in *en-Gal4/+* control wing imaginal discs and *en-Gal4; UAS-rbf1* wing imaginal discs. In posterior compartment, *rbf1* overexpression slightly alter the  $\beta$ -Gal staining aspect as compared with the *en-gal4/+* control (Figures 3a and b), probably due to the presence of apoptotic cells, but we could not observe a real staining decrease. Nevertheless, Diap1 protein had decreased in the posterior compartment upon *rbf1* overexpression (Figure 3d). These data suggest that *rbf1* overexpression would induce a post-transcriptional reduction of *diap1* mRNA.

Interestingly, it has been reported that *diap1* is a target of How, an RNA-binding protein that belongs to the STAR family.<sup>36</sup> Two How isoforms have been described. The short isoform, How(S), is involved in mRNA stability and splicing.<sup>37</sup> The long isoform, How(L), binds the 3'UTR of target mRNAs, leading to their destabilization and their rapid degradation. *diap1* is a target of How(L).<sup>36</sup> We used *how<sup>stru</sup>* loss-of-function mutant to determine the implication of How in Rbf1-induced apoptosis. When *rbf1* was overexpressed in a *how<sup>stru</sup>* heterozygous context, distribution of the phenotypes significantly shifted toward weaker phenotypes as compared with the expression of *rbf1* alone. Consistently, the number of

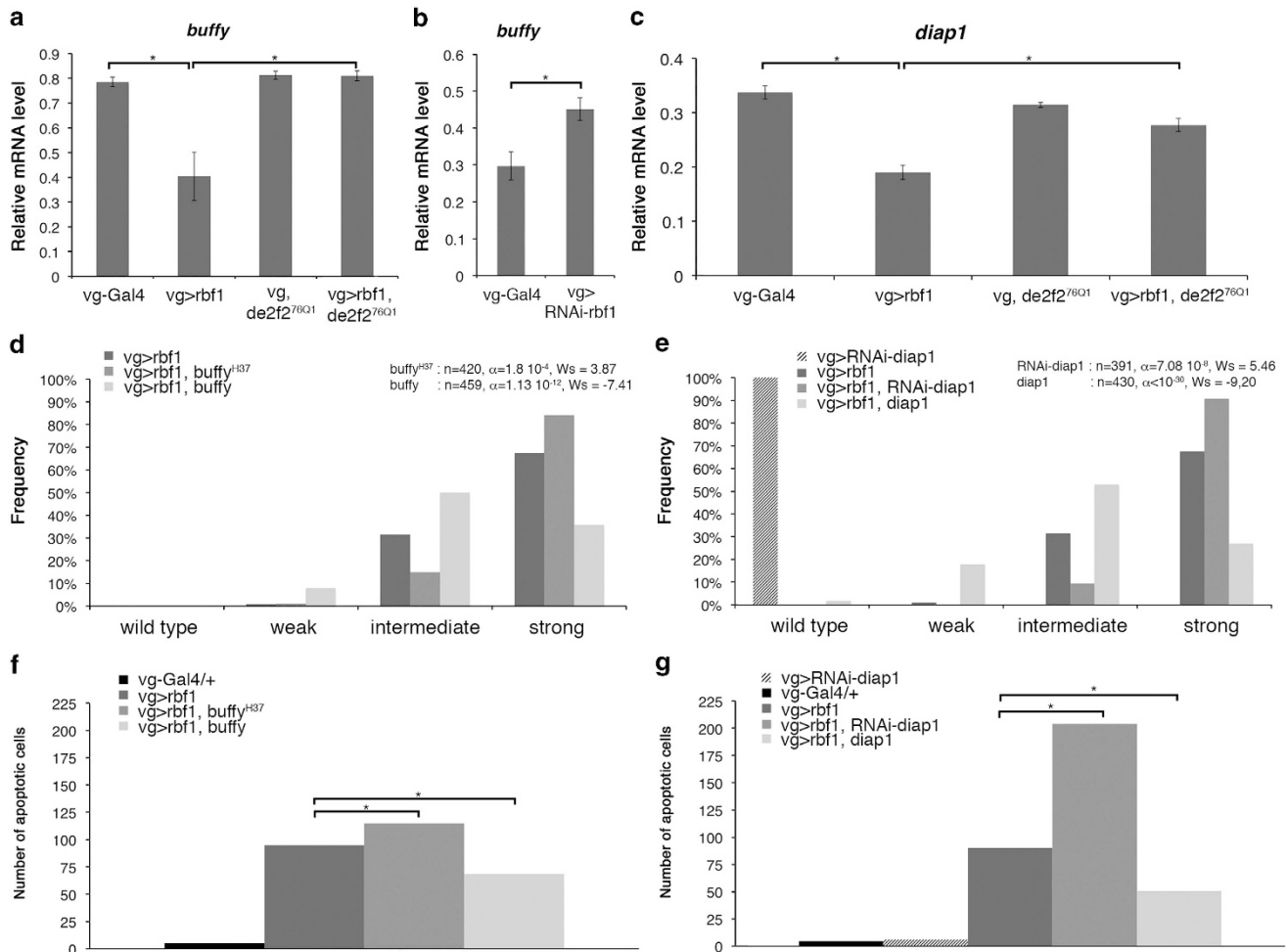


**Figure 2** *rbf1* overexpression induces downregulation of *buffy* and *diap1* mRNA. (a–c) Quantification of *buffy* (a, b) and *diap1* (c) mRNA by RT-qPCR in wing imaginal discs. Data are normalized against *rp49* and correspond to the mean of three independent experiments. Error bars are the S.E.M. Asterisks indicate statistical significant difference between two genotypes (Student's *t*-test,  $P < 0.05$ ). (d, e) Distribution of notches in wings of *vg-Gal4 > UAS-rbf1*, *vg-Gal4 > UAS-rbf1; buffy<sup>H37</sup>* and *vg-Gal4 > UAS-rbf1; UAS-buffy* flies (d), *vg-Gal4 > UAS-rbf1*, *vg-Gal4 > UAS-rbf1; UAS-RNAi-diap1* and *vg-Gal4 > UAS-rbf1; UAS-diap1* flies (e). Wing phenotypes were grouped in four categories according to the number of notches (wild type, weak, intermediate, strong). Statistical analysis was performed using Wilcoxon tests. Each experiment was independently performed three times; as the results were similar, only one experiment is presented here. (f, g) Quantification of TUNEL-positive cells in the wing pouch. Asterisks indicate a statistically significant difference between two genotypes (Student's *t*-test,  $P < 0.05$ )

apoptotic cells decreased in wing imaginal discs of the same genotype (Figures 3e and f). Thus, How is necessary for Rbf1-induced apoptosis. To confirm that How is involved in *diap1* regulation, we performed RT-qPCR. In *how<sup>stru</sup>* heterozygotes, *diap1* mRNA were slightly but significantly decreased indicating that How is required to maintain a basal level of *diap1* mRNA (Figure 3g). When *rbf1* was overexpressed in a *how<sup>stru</sup>* heterozygous context, *diap1* mRNA increased as compared with the *rbf1* overexpression alone and even exceeded the level observed in *vg-Gal4/+* control. Therefore, these data suggest that Rbf1-induced apoptosis leads to *diap1* mRNA destabilization by How.

To confirm whether *diap1* downregulation by How in Rbf1-induced apoptosis involved *diap1* 3'UTR, we performed a genetic interaction test using a *UAS-diap1<sup>UY1835</sup>* transgenic line. This line bears a *P* element in the 5'UTR sequence of the *diap1* gene, which allows overexpressing *diap1* with its 3'UTR sequence.<sup>38</sup> Contrary to the phenotypic rescue

observed when *rbf1* was co-overexpressed with *diap1* devoid of its 3'UTR sequence (Figure 2e), *rbf1* co-overexpression with *diap1<sup>UY1835</sup>* did not lead to a rescue of notch phenotypes (Figure 3h). Interestingly, *diap1<sup>UY1835</sup>* allowed an effective increase in the Diap1 protein level as attested by Diap1 immunostaining (Figure 3j); however, this protein level was significantly lower when *rbf1* was overexpressed (Figure 3k). This suggests that Diap1 cannot accumulate in an *rbf1*-overexpressing context. When *rbf1* and *diap1<sup>UY1835</sup>* were co-overexpressed in a *how<sup>stru</sup>* heterozygous context, the Diap1 protein accumulated (Figure 3l) and consistently, we observed a significant rescue as compared with the expression of *rbf1* in a *how<sup>stru</sup>* mutant context (Figure 3h, Wilcoxon test:  $n = 308$ ,  $\alpha < 10^{-30}$ , Ws = -8.95). The variation of the phenotypic distribution between these different genetic contexts correlated with a variation of the amount of apoptosis in wing imaginal discs (Figure 3m). Thus, the *how<sup>stru</sup>* heterozygote context prevents *diap1* repression by



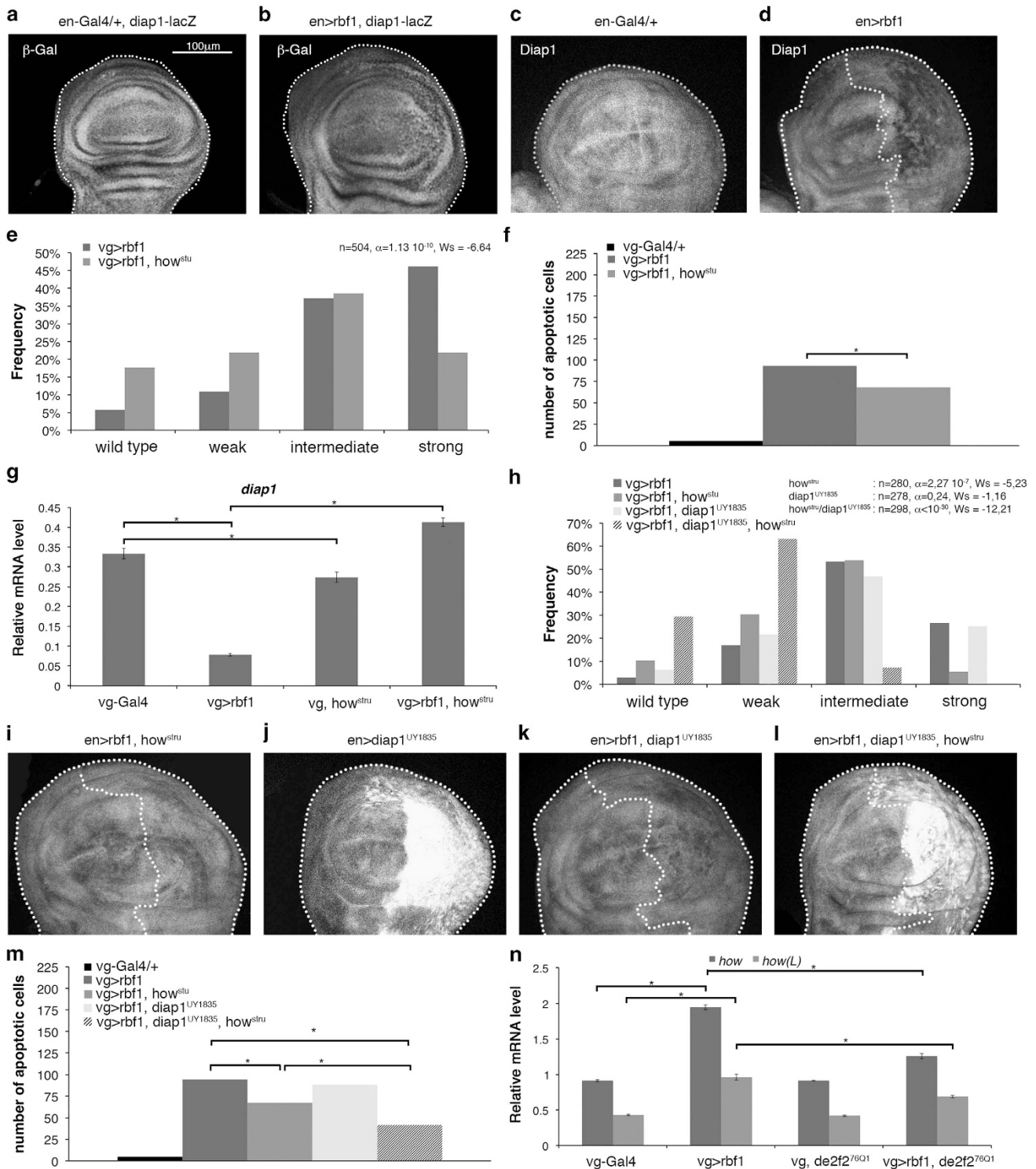


**Figure 3** Rbf1 and dE2F2 increases *how* mRNA leading to *diap1* mRNA destabilization. (a) *diap1-lacZ* transgene was used to report *diap1* transcription in *en-gal4/+* and *en-gal4 > UAS-rbf1* genetic contexts.  $\beta$ -Gal immunostaining (white) of the discs are shown in (a, b). Diap1 immunostaining (white) are shown in (c, d) and (i–l). The genotypes are indicated at the top of the image. Posterior compartment of the wing disc (on the right) is delimited by dotted line when *rbf1* is overexpressed. All the pictures presented in Figure 3 are at the same scale, scale bar: 100  $\mu$ m. Distribution of notch wing phenotypes in *vg-Gal4 > UAS-rbf1* and *vg-Gal4 > UAS-rbf1; how<sup>stru</sup>* flies (e), *vg-Gal4 > UAS-rbf1, how<sup>stru</sup>*, *vg-Gal4 > UAS-rbf1; UAS-diap1<sup>UY1835</sup>* and *vg-Gal4 > UAS-rbf1; UAS-diap1<sup>UY1835</sup>, how<sup>stru</sup>* flies (h). Wing phenotypes were grouped into four categories according to the number of notches (wild type, weak, intermediate, strong). Statistical analysis was performed using Wilcoxon tests. Each experiment was independently performed three times; as the results were similar, only one experiment is presented here. Quantification of TUNEL-positive cells (f and m) in the wing pouch of genotypes studied in (e) and (h). Asterisks indicate a statistically significant difference between two genotypes (Student's *t*-test,  $P < 0.05$ ). Quantification of *diap1* (g), *how* and *how(L)* (n) mRNAs in wing imaginal discs by RT-qPCR. Data are normalized against *rp49* and correspond to the mean of three independent experiments. Error bars are the S.E.M. Asterisks indicate statistically significant difference between two genotypes (Student's *t*-test,  $P < 0.05$ )

Rbf1. These results indicate that *diap1* downregulation by Rbf1 requires both the *diap1* 3'UTR sequence and How. We next asked whether *rbf1* overexpression could affect the expression of *how(L)*. Indeed, *how(L)* mRNA increased on *rbf1* overexpression (Figure 3n). Surprisingly, this raise depended on dE2F2 as it was reduced in a *de2f2*<sup>76Q1</sup> heterozygous context. This could be explained by an indirect effect of dE2F2, or by an unusual transcriptional activity of dE2F2. Thus, these data suggest that Rbf1 and dE2F2 increase of *how(L)* mRNA leads to destabilization of *diap1* mRNA that induces apoptosis.

**Rbf1 and dE2F2 binds *buffy* and *how* genomic regions near the TSSs.** As the 5' UTR of *buffy* contains dE2F2 binding sites, we performed chromatin immunoprecipitation (ChIP) experiments to determine whether Rbf1 and dE2F2 directly bound this region. We used *pcna*, a well-characterized target of Rbf1/dE2F complexes, as a positive control and *slp1*, a nontarget gene of Rbf1,<sup>39</sup> as a negative control. No significant enrichment was observed of the negative control *slp1* after Rbf1 or dE2F2 immunoprecipitation (IP). In contrast, we detected a significant enrichment of the positive control *pcna* promoter region on Rbf1 or dE2F2 IP as compared with the mock IP (Figures 4a and b). The *buffy* 5'UTR was significantly enriched after Rbf1 and dE2F2 IPs as compared with the negative controls both in *rbf1*-overexpressing wing discs and control discs (Figures 4a and b). Therefore, Rbf1 and dE2F2 bound *buffy* in the wing imaginal discs. Then, Rbf1 and dE2F2 might directly repress *buffy* transcription.

The *how* promoter also contains a putative dE2F binding site suggesting that Rbf1 and dE2F2 could bind this region. Consistently, we observed that *how* genomic region was significantly enriched after both Rbf1 and dE2F2 IP in *rbf1*-overexpressing wing discs (Figures 4a and b). Nevertheless, these enrichments were not observed with the control discs. Despite the fact that Rbf1/dE2F2 complex is almost exclusively described as a transcriptional repressor, our results suggest that Rbf1 and dE2F2 might directly activate *how* transcription.

**Transcriptional control by different members of the dREAM complex depends on the target gene.** Rbf1 and dE2F2 belong to a multi-subunit complex named dREAM. This complex positively regulates some target genes, whereas it negatively regulates some others. Certain proteins of the complex are activators, whereas others are repressors or not involved. Moreover the role of each protein can change according to the target gene. To determine the function of the dREAM subunits Mip120, Mip130 and Myb in Rbf1-induced apoptosis, we performed genetic interaction tests. When *rbf1* was co-overexpressed with either *RNAi-mip120* or *RNAi-mip130*, the distribution of wing phenotypes shifted toward weaker phenotypes as compared with the expression of *rbf1* alone (Figures 5a and b). Consistently, the number of apoptotic cells decreased in the wing discs of the same genotypes (Figures 5d and e), indicating that Mip120 and Mip130 were necessary for Rbf1-induced apoptosis.

*rbf1* and *myb* co-expression induces a shift in the phenotype distribution toward weaker phenotypes (Figure 5c) and a decrease of apoptotic cells (Figure 5f). Therefore, Myb is sufficient to inhibit Rbf1-induced apoptosis. This result is in an agreement with the antagonistic role of Myb as compared with the role of other members of the complex, previously described.<sup>30</sup>

We next assessed the contribution of Mip120, Mip130 and Myb to *buffy* and *how* transcriptional regulation by RT-qPCR. Depletion of Mip120 or Mip130 by *RNAi* induced an increase of *buffy* mRNA as compared with *vg-Gal4/+* control (Figure 5g), indicating that Mip120 and Mip130 are required to repress *buffy* expression in the wing imaginal discs. Moreover, when *rbf1* was co-overexpressed with *RNAi-mip120*, *buffy* mRNA increased as compared with the *rbf1* expression alone. Similar results were observed with *RNAi-mip130*, indicating that these two genes are required for Rbf1 to repress *buffy* expression. Depletion of Myb by *RNAi* did not affect *buffy* expression, whereas *myb* overexpression increased it (Figure 5h). Furthermore, when *rbf1* and *myb* were co-overexpressed, the amount of *buffy* mRNA was similar to the one of *vg-Gal4/+* control. Thus, Myb and Mip proteins had opposite roles on *buffy*

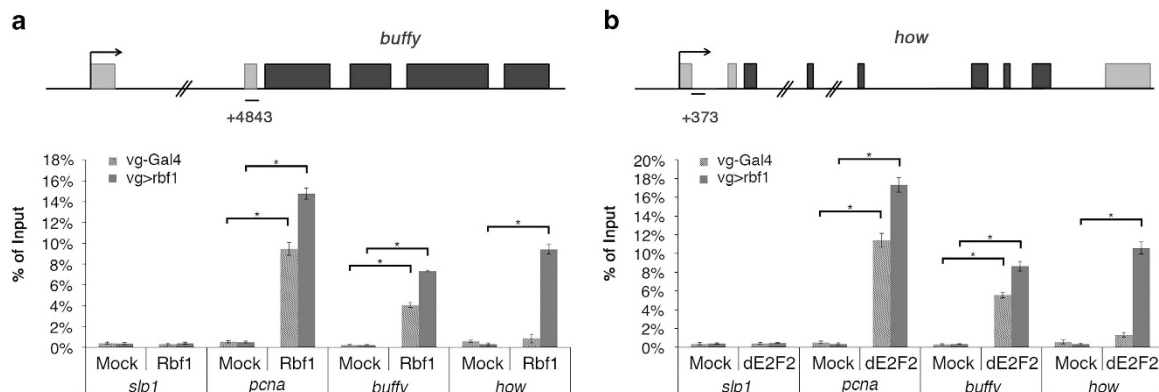


**Figure 4** Binding of Rbf1 and dE2F2 on *buffy* and *how* genes. Structure of *buffy* (a) and *how* (b) genes. qPCR amplicons are indicated. Coordinated of qPCR amplicons relative to TSS are indicated. ChIP-qPCR analysis of *buffy* (a) and *how* (b) from *vg-gal4 > UAS-Rbf1* or control (*vg-Gal4/+*) wing imaginal discs using mock, anti-Rbf1 or anti-dE2F2 antibodies. The results were expressed as percentages of input. *slp1*, a nontarget gene of Rbf1, was used as a negative control whereas *pcna*, a known dE2Fs target, was used as a positive control. Error bars represent S.E.M obtained from three independent experiments. Asterisks indicate statistically significant difference between two genotypes (Student's *t*-test,  $P < 0.05$ )

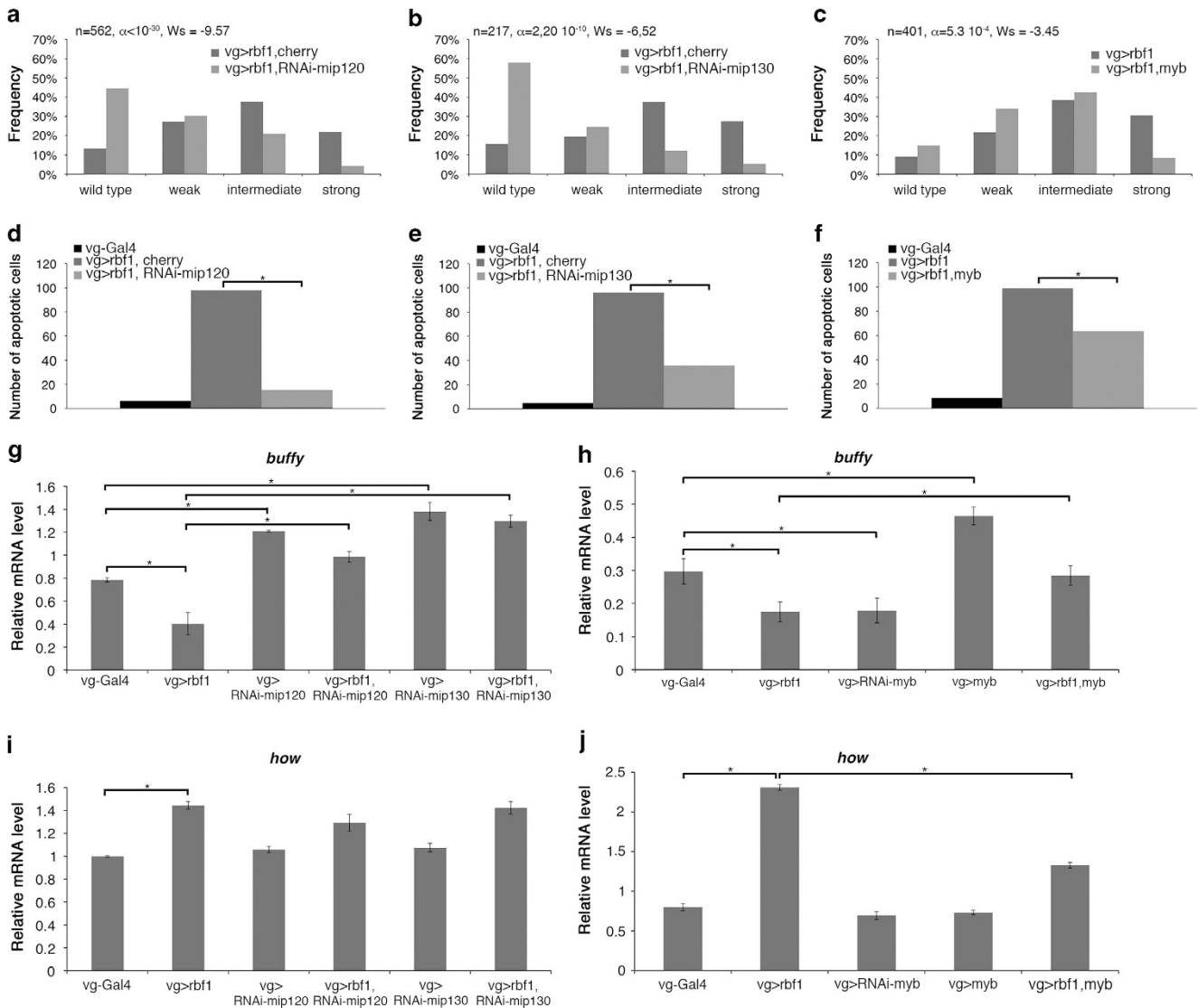


**Figure 5** Mip proteins and Myb are differentially involved in Rbf1-induced apoptosis. (a–c) Distribution of notch wing phenotypes in *vg-Gal4 > UAS-rbf1, UAS-cherry* and *vg-Gal4 > UAS-rbf1, UAS-RNAi-mip120* (a), in *vg-Gal4 > UAS-rbf1, UAS-cherry* and *vg-Gal4 > UAS-rbf1; UAS-RNAi-mip130* (b) and in *vg-Gal4 > UAS-rbf1* and *vg-Gal4 > UAS-rbf1; UAS-myb* (c). Wing phenotypes were grouped in four categories according to the number of notches (wild type, weak, intermediate, strong). Statistical analysis was performed using Wilcoxon tests. Each experiment was independently performed three times; as the results were similar, only one experiment is presented here. (d–f) Quantification of TUNEL-positive cells in the wing pouch of genotypes studied in (a–c). Asterisks indicate a statistically significant difference between two genotypes (Student’s *t*-test,  $P < 0.05$ ). (g–j) Quantification of *buffy* (g, h) and *how* (i, j) mRNA in wing imaginal discs by RT-qPCR. Data are normalized against *rp49* and correspond to the mean of three independent experiments. Error bars are the S.E.M. Asterisks indicate statistically significant difference between two genotypes (Student’s *t*-test,  $P < 0.05$ ).

transcriptional regulation: whereas Myb activated *buffy* transcription, Mip factors repressed it.

Inactivation of *Mip120* or *Mip130* by *RNAi* did not affect the basal level of *how* mRNA (Figure 5i). Moreover, when *rbf1* was co-overexpressed with either *RNAi-mip120* or *RNAi-mip130*, the amount of *how* mRNA was similar to the one observed for *rbf1* overexpression alone, suggesting that these Mip factors are not involved in the transcriptional regulation of *how* by Rbf1.

Inactivation or overexpression of *myb* did not alter the basal amount of *how* mRNA (Figure 5j). However, *rbf1* and *myb* co-overexpression decreased the level of *how* mRNA as compared with the *rbf1* overexpression alone. These data suggest that, contrary to dE2F2, Myb antagonizes Rbf1-induced *how* transcriptional activation.

## Discussion

E2F transcription factors are the main partners of Rbf1. dE2F1 is widely described for its important role in the control of cell proliferation by Rbf1, whereas the best-described role of dE2F2 is the repression of replication during oogenesis.<sup>35,40</sup> Here, we show that dE2F2 and dDP are required for Rbf1-induced apoptosis suggesting that they are pro-apoptotic factors, contrary to dE2F1, which inhibits this apoptosis. Until now, dE2F1 was mainly described as a pro-apoptotic factor, whereas dE2F2 was most of the time described as an anti-apoptotic factor. Indeed, *de2f1* and *dDp* co-expression induces apoptosis in the eye imaginal discs<sup>23</sup> and dE2F1 promotes irradiation-induced Dp53-independent apoptosis in wing

imaginal discs, whereas dE2F2 inhibits apoptosis in the same model.<sup>41</sup> Recently, Rovani *et al.*<sup>42</sup> showed that the dREAM complex, which includes dE2F2, cooperates with the pro-apoptotic factor Grim to induce cell death in the peripheral nervous system. This result suggests a pro-apoptotic role for dE2F2, which is consistent with our results. Furthermore, the role of dE2F1 in apoptosis might depend on the cellular context. Indeed, dE2F1 is important for DNA damage-induced apoptosis in the wing imaginal discs, but its role varies depending on the position of the cell within the disc.<sup>43</sup> Together, this result and ours indicate that the role of both dE2F1 and dE2F2 in apoptosis control depends on the cellular context. Similarly, depending on the cells or tissues, Rbf1 has a pro- or anti-apoptotic effect. Indeed, RBF expression induces apoptosis in different proliferative tissues, whereas this effect was not observed in differentiated post-mitotic cells.<sup>26</sup>

RNAi-based studies suggested a requirement of *buffy* for cell survival during embryonic development.<sup>44</sup> Another study suggests that *Buffy* is not involved in developmental cell death but modulates the response to irradiation-induced cell death.<sup>45</sup> Here, we show that *buffy* is involved in apoptosis induced by overexpression of the tumor suppressor gene *rbf1*. Furthermore, our data reveal for the first time that Rbf1 regulates *buffy* transcription. It would thus be interesting to determine whether Rbf1 also regulates *buffy* in response to irradiation.

At least in some cancers, pRb oncosuppressor activity relies on its apoptosis-inducing activity. It has been suggested that RB mutations can affect the sensitivity to mitomycin/anthracycline treatment in breast cancer.<sup>46</sup> Several reports underline the importance of pRb in the apoptotic response of prostate cancer cells to radiotherapy or chemotherapeutic drugs.<sup>11,12,47</sup> How pRb mediates apoptosis in these cases remains unclear. Other data show that DNA damage promotes the formation of a pRB/E2F1 complex involved in the activation of pro-apoptotic genes such as *Caspase 7* and

*p73*,<sup>13</sup> and that RB/E2F-1 is a major contributor of *Noxa* induction in response to ABT-737 treatment, a Bcl-2 inhibitor.<sup>48</sup> Thus, pRB/E2F proapoptotic signaling(s) can be activated in response to oncogenic stress, DNA damage or Bcl-2 inhibition. Similarly, our data show that in *Drosophila*, Rbf1/dE2F2 can regulate apoptosis by upregulating *how* (Figure 6). Although this regulation seems non-essential to maintain the *how* mRNA basal level, we cannot exclude that it occurs in response to some stresses and/or therapeutic treatments. Indeed, *Quaking*, the homolog of *how*, has been shown to be a tumor suppressor.<sup>49–51</sup> It would be interesting to study whether a pRB/E2F complex can regulate a mammalian homolog of the *DIAP1* gene via *Quaking*.

Rbf1 and dE2F2 belong to a large complex called dREAM. Inactivation of members of dREAM by RNAi in Kc cells leads to variations of *how* and *buffy* expression,<sup>32</sup> which suggests that these two genes could be direct transcriptional targets of dREAM. Such as described by Georgette *et al.*,<sup>32</sup> we found that the involvement of dREAM complex members are not equivalent: some members can be activators for a specific target, whereas others are repressors or are not involved in transcriptional regulation of this target. Indeed dE2F2, Mip120 and Mip130 are required for Rbf1-induced transcriptional repression of *buffy*, whereas Myb has an opposite effect. Moreover, contrary to dE2F2 and Myb, Mip120 and Mip130 are not involved in *how* regulation.

dE2F2 and Myb have opposite effects on Rbf1-induced *buffy* and *how* transcription. Our results are in agreement with transcriptomic data indicating that there are no genes negatively co-regulated by Myb and dE2F2 but many genes are regulated both positively by Myb and negatively by dE2F2.<sup>32</sup>

Our results confirm a previous report<sup>32</sup> indicating that Rbf1 and the dREAM complex can act both as a transcriptional activator and as a transcriptional repressor (Figure 6). The molecular mechanisms for transcriptional repression have

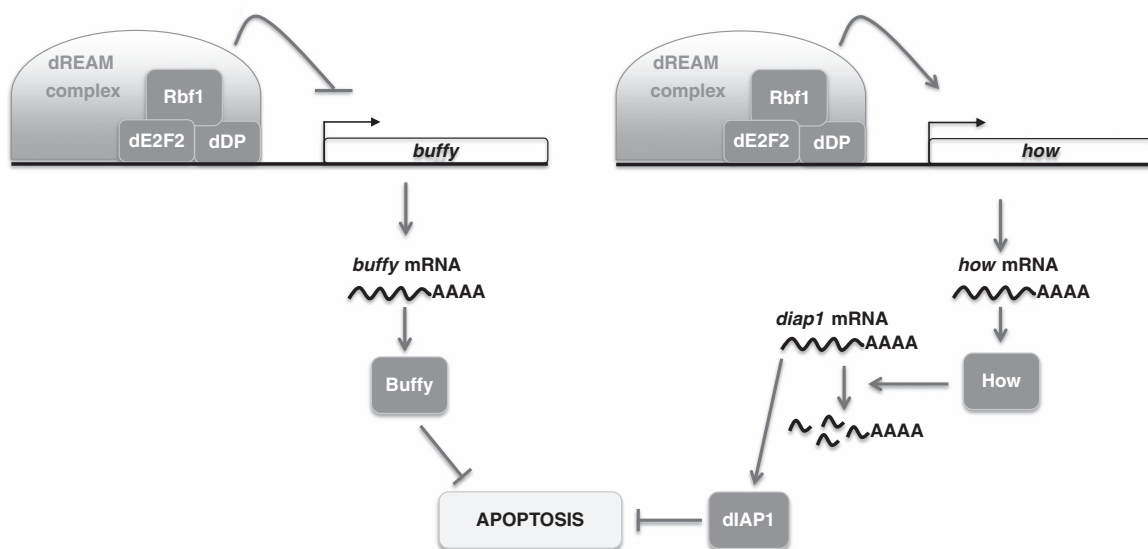


**Figure 6** Rbf1-induced apoptosis involved transcriptional regulation of *buffy* and *how* genes. Rbf1 with dE2F2 binds *buffy* genomic site near to TSS and represses its transcription. The decrease of *buffy* mRNA contributes to Rbf1-induced apoptosis. Rbf1 can also bind *how* promoter with dE2F2 but this time it induces a transcriptional upregulation. As a consequence, *How* level increases allowing *diap1* mRNA degradation which promotes Rbf1-induced cell death. Some members of the dREAM complex are involved in these transcriptional regulations



been deciphered.<sup>31</sup> It would be interesting to determine which epigenetic mechanisms are involved in the transcriptional activation of dREAM complex target genes.

Using an overexpression system, we have identified the *bcl-2* family gene *buffy*, as a transcriptional target of Rbf1. In an *rbf1* loss-of-function mutant, *buffy* transcription increases show that in wild-type cells not committed to apoptosis, Rbf1 is necessary to limit *buffy* expression. Thus, *rbf1* loss of function could render cells more resistant to apoptosis. Identification of *buffy* as an Rbf1/dE2F pathway target gene is consistent with the role of tumor suppressor described for the human counterpart Rb. Transcriptional regulation of *bcl-2* family genes by Rb/E2F complexes has also been characterized in mammals. Indeed, pRb/E2F1 directly regulates *nox4*,<sup>48</sup> *bim*<sup>52</sup> and *puma*.<sup>53</sup> Regulation by Rb of *bcl-2* family gene expression may have a major impact on cell death and can thus contribute to its tumor suppressor action.

## Materials and Methods

**Fly stocks.** Flies were raised at 25 °C on a standard medium. The *UAS-Rbf1* and *vg-Gal4* strains were generous gifts from J Silber. The *en-Gal4* strain was kindly provided by L Théodore. The *UAS-diap1* strain was a generous gift from A-M Pret. In this strain, a transgene containing *diap1* cDNA under the control of a UAS sequence is inserted on the second chromosome and allows the expression of *diap1* without its 3'UTR sequence. The *UAS-diap1*<sup>UY1835</sup> was a kind gift from S Netter.<sup>38</sup> In this transgenic line, a *P* element is inserted in the 5'UTR sequence of *diap1* gene in the correct orientation to allow the expression of *diap1* with its 3'UTR sequence. The following strains were obtained from the Bloomington Stock Center (Bloomington, IN, USA): *dE2F2*<sup>76Q1</sup> (7436), *UAS-dE2F2* (17314), *dDp*<sup>a1</sup> (7277), *dE2F1*<sup>2</sup> (7274), *buffy*<sup>H37</sup> (27340), *UAS-buffy* (32059), *diap1-lacZ* (12093), *how*<sup>stru</sup> (2301), *UAS-RNAi-mip120* (32461), *UAS-RNAi-mip130* (32462), *UAS-RNAi-myb* (35053), *UAS-myb* (32044). The *UAS-RNAi-diap1* strain was from NIG collection (12284R-2). The *UAS-RNAi-rbf1* strain was from VDRC collection (10696).

**Test of phenotype suppression in the wing.** To test the implication of several genes (*dE2F1*, *dE2F2*, *dDP*, *Buffy*, *Diap1*, *How*, *Mip120*, *Mip130* and *Myb*) in *rbf1*-induced apoptosis, the severity of the notched wing phenotype induced by *UAS-Rbf1* overexpression led by *vg-Gal4* driver was assayed in different genetic contexts. For each gene, we verified that the alteration of this gene expression level (overexpression, RNAi or mutant) did not induce any wing phenotype. *vg-Gal4 > UAS-Rbf1* *Drosophila* females were crossed with males bearing a loss-of-function mutation for the different genes or allowing their overexpression. The progenies of all crosses were classified according to the number of notches on the wing margin. Wilcoxon tests were performed as described previously.<sup>54</sup>

**TUNEL staining of imaginal discs.** Third instar larvae were dissected in PBS pH 7.6, fixed in PBS/formaldehyde 3.7%, washed three times for 10 min in PBT (1 × PBS, 0.5% Triton). Discs were then dissected and TUNEL staining was performed according to manufacturer's instructions (ApoTag Red *in situ* apoptosis detection kit, Millipore, Temecula, CA, USA). Discs were mounted in CitifluorTM (Biovalley, Marne-La-Vallée, France) and observed with a Leica SPE upright confocal microscope (Leica, Wetzlar, Germany). White patches in the wing pouch were counted for at least 30 wing imaginal discs per genotype. Student's *t*-tests were performed and results were considered to be significant when  $\alpha < 5\%$ .

**Immunocytochemistry.** The following antibodies were used: anti- $\beta$ -Gal (mouse monoclonal antibody, 1/200, 40-1a, DSHB) and anti-Diap1 (mouse monoclonal antibody, 1/200, generous gift from B Hay). Third instar larvae were dissected in PBS pH 7.6, fixed in PBS-3.7% formaldehyde, washed three times for 10 min each in PBT (PBS, 0.3% Triton) and incubated with primary antibody overnight at 4 °C in PBT-FCS (PBS, 0.3% Triton, 10% FCS). Incubation with anti-mouse secondary antibody (Alexa Fluor 488 Goat Anti-Mouse IgG (H+L) Antibody, Molecular Probes, Thermo Fisher Scientific, Waltham, MA, USA) was carried in PBT-FCS for 2 h at room temperature. Larvae were then washed thrice in PBT. Finally, wing discs were mounted in CitifluorTM (Biovalley) and observed with a Leica SPE upright confocal microscope.

**Chromatin immunoprecipitation.** ChIPs were performed as previously described,<sup>55</sup> with minor modification. Briefly, 50 *vg-Gal4 > UAS-rbf1* wing imaginal discs of third instar larvae were dissected on ice in serum-free Schneider medium. They were fixed in 500  $\mu$ l of formaldehyde (1.8% in PBS) for 10 min at room temperature under gentle agitation. Cross-linking was stopped by adding 50  $\mu$ l of glycine 1.25 M. Fixed wing discs were washed 3 times with PBS, dried, flash-frozen in liquid nitrogen and stored at -80 °C. Cell lysis was performed by adding 100  $\mu$ l of lysis buffer (140 mM NaCl, 10 mM Tris-HCl pH 8.0, 1 mM EDTA, 1% Triton X-100, 0.1% sodium deoxycholate, Roche complete EDTA-free protease inhibitor cocktail) complemented with 1% SDS and sonicated in a Bioruptor sonifier (Diagenode, Seraing, Belgium). Conditions were established to obtain chromatin fragments from 200 to 1000 bp in length (30 s ON 30 s OFF, high power, 10 cycles). Pooled chromatin was centrifuged for 20 min at 14 000 *g* at 4 °C. The supernatant (soluble chromatin) was recovered and 10  $\mu$ l were kept as input sample. For each IP, 10  $\mu$ l of protein A-coated paramagnetic beads (Diagenode) were washed once in lysis buffer, 1  $\mu$ g of antibody was added and beads were incubated for 2 h at 4 °C on a rotating wheel. After washing in lysis buffer, antibody coated beads were resuspended in 300  $\mu$ l of lysis buffer and 100  $\mu$ l of chromatin were added. After incubation on a rotating wheel overnight at 4 °C, beads were washed at 4 °C five times for 10 min each in lysis buffer, once in LiCl buffer (Tris-HCl 10 mM pH8.0, LiCl 0.25 M, 0.5% NP-40, 0.5% sodium deoxycholate, 1 mM EDTA) and twice in TE (10 mM Tris-HCl, pH 8.0, 1 mM EDTA). Immunoprecipitated as well as input DNAs were purified with the IPure kit following the manufacturer's instructions (Diagenode). Elution was performed twice with 35  $\mu$ l of water. 5  $\mu$ l of DNA were used per PCR. Real-time PCR data were normalized against the input sample and depicted as percentage of input (see Supplementary Table S1 for primers). *pcna*, a well characterized target of Rbf1/dE2F complexes, was used as a positive control and *slp1*, a nontarget gene of Rbf1,<sup>39</sup> as a negative control.

Antibodies used for chromatin immunoprecipitation were anti-Rbf1 (rabbit polyclonal, Custom antibody against amino acids 250-845 of Rbf1 protein, Proteogenix, Schiltigheim, France), anti-dE2F2 (rabbit polyclonal, Custom antibody against the whole protein, Proteogenix). Rabbit pre-immune sera were used as negative controls (mocks).

**RNAs extraction and RT-qPCR.** Fifty wing imaginal discs per genotype were dissected on ice in serum-free Schneider medium. Total RNAs were extracted from each sample using the RNeasy Mini kit (Qiagen, Venlo, Netherlands), by following the manufacturer's instructions. RT was performed on each sample using 4.8  $\mu$ g of RNA incubated with random primer oligonucleotides (Invitrogen, Life Technologies, Carlsbad, CA, USA) with Recombinant Taq DNA Polymerase (Invitrogen), according to the manufacturer's instructions.

Real-time PCR analysis was performed using the ABI Prism 7700 HT apparatus (Applied Biosystems, Life Technologies). Briefly, PCR was performed with the Absolute blue QPCR SYBR Green ROX mix (Abgene, Thermo Fisher Scientific), using 11 ng of cDNA per RT. The primers used for real-time PCR are presented in Supplementary Table S2. Data were normalized against *rp49*. Three independent RT experiments were performed and the S.E.M was calculated from these three independent samples.

## Conflict of Interest

The authors declare no conflict of interest.

**Acknowledgements.** We are grateful to S Szuplewski, S Gaumer and F Peronnet for their critical reading of the manuscript. We thank B Hay for a generous gift of dIAP1 antibody. Confocal microscopy was performed on CYMAGES imaging facility. qPCR experiments were done in the UMR 1198 'Biologie du Développement et Reproduction' (INRA, Jouy-en-Josas). This work was supported by the 'Université de Versailles Saint-Quentin-en-Yvelines' (UVSQ) and by grants from the 'Ligue Nationale Contre le Cancer'. Amandine Clavier was the recipient of a doctoral contract from UVSQ. Adrienne Baillet was supported by the UVSQ and the Ecole Pratique des Hautes Etudes.

1. van den Heuvel S, Dyson NJ. Conserved functions of the pRB and E2F families. *Nat Rev Mol Cell Biol* 2008; 9: 713–724.
2. Frolov MV, Dyson NJ. Molecular mechanisms of E2F-dependent activation and pRB-mediated repression. *J Cell Sci* 2004; 117: 2173–2181.

3. Almasan A, Yin Y, Kelly RE, Lee EY, Bradley A, Li W *et al*. Deficiency of retinoblastoma protein leads to inappropriate S-phase entry, activation of E2F-responsive genes, and apoptosis. *Proc Natl Acad Sci USA* 1995; **92**: 5436–5440.
4. Knudsen KE, Booth D, Naderi S, Sever-Chroneos Z, Fribourg AF, Hunton IC *et al*. RB-dependent S-phase response to DNA damage. *Mol Cell Biol* 2000; **20**: 7751–7763.
5. Clarke AR, Maandag ER, van Roon M, van der Lugt NM, van der Valk M, Hooper ML *et al*. Requirement for a functional Rb-1 gene in murine development. *Nature* 1992; **359**: 328–330.
6. Jacks T, Fazeli A, Schmitt EM, Bronson RT, Goodell MA, Weinberg RA. Effects of an Rb mutation in the mouse. *Nature* 1992; **359**: 295–300.
7. Lee EY, Chang CY, Hu N, Wang YC, Lai CC, Herrup K *et al*. Mice deficient for Rb are nonviable and show defects in neurogenesis and haematopoiesis. *Nature* 1992; **359**: 288–294.
8. Tsai KY, Hu Y, Macleod KF, Crowley D, Yamasaki L, Jacks T. Mutation of E2F-1 suppresses apoptosis and inappropriate S phase entry and extends survival of Rb-deficient mouse embryos. *Mol Cell* 1998; **2**: 293–304.
9. Huh MS, Parker MH, Scime A, Parks R, Rudnicki MA. Rb is required for progression through myogenic differentiation but not maintenance of terminal differentiation. *J Cell Biol* 2004; **166**: 865–876.
10. Biasoli D, Kahn SA, Cornelio TA, Furtado M, Campanati L, Chneiweiss H *et al*. Retinoblastoma protein regulates the crosstalk between autophagy and apoptosis, and favors glioblastoma resistance to etoposide. *Cell Death Dis* 2013; **4**: e767.
11. Zhao X, Day ML. RB activation and repression of C-MYC transcription precede apoptosis of human prostate epithelial cells. *Urology* 2001; **57**: 860–865.
12. Bowen C, Spiegel S, Gelmann EP. Radiation-induced apoptosis mediated by retinoblastoma protein. *Cancer Res* 1998; **58**: 3275–3281.
13. Ianari A, Natale T, Calo E, Ferretti E, Alessi E, Screpani I *et al*. Proapoptotic function of the retinoblastoma tumor suppressor protein. *Cancer Cell* 2009; **15**: 184–194.
14. Hilgendorf KI, Leshchiner ES, Nedelcu S, Maynard MA, Calo E, Ianari A *et al*. The retinoblastoma protein induces apoptosis directly at the mitochondria. *Genes Dev* 2013; **27**: 1003–1015.
15. Dynlacht BD, Brook A, Dembski M, Yenush L, Dyson N. DNA-binding and trans-activation properties of Drosophila E2F and DP proteins. *Proc Natl Acad Sci USA* 1994; **91**: 6359–6363.
16. Ohtani K, Nevins JR. Functional properties of a Drosophila homolog of the E2F1 gene. *Mol Cell Biol* 1994; **14**: 1603–1612.
17. Sawado T, Yamaguchi M, Nishimoto Y, Ohno K, Sakaguchi K, Matsukage A. dE2F2, a novel E2F-family transcription factor in Drosophila melanogaster. *Biochem Biophys Res Commun* 1998; **251**: 409–415.
18. Du W, Vidal M, Xie JE, Dyson N. RBF, a novel RB-related gene that regulates E2F activity and interacts with cyclin E in Drosophila. *Genes Dev* 1996; **10**: 1206–1218.
19. Stevaux O, Dimova D, Frolov MV, Taylor-Harding B, Morris E, Dyson N. Distinct mechanisms of E2F regulation by Drosophila RBF1 and RBF2. *EMBO J* 2002; **21**: 4927–4937.
20. Du W. Suppression of the rbf null mutants by a de2f1 allele that lacks transactivation domain. *Development* 2000; **127**: 367–379.
21. Frolov MV, Huen DS, Stevaux O, Dimova D, Balczarek-Strang K, Elsdon M *et al*. Functional antagonism between E2F family members. *Genes Dev* 2001; **15**: 2146–2160.
22. Du W, Dyson N. The role of RBF in the introduction of G1 regulation during Drosophila embryogenesis. *EMBO J* 1999; **18**: 916–925.
23. Du W, Xie JE, Dyson N. Ectopic expression of dE2F and dDP induces cell proliferation and death in the Drosophila eye. *EMBO J* 1996; **15**: 3684–3692.
24. Asano M, Nevins JR, Wharton RP. Ectopic E2F expression induces S phase and apoptosis in Drosophila imaginal discs. *Genes Dev* 1996; **10**: 1422–1432.
25. Zhou L, Steller H. Distinct pathways mediate UV-induced apoptosis in Drosophila embryos. *Dev Cell* 2003; **4**: 599–605.
26. Millet C, Rincheval-Arnold A, Mignotte B, Guenal I. The Drosophila retinoblastoma protein induces apoptosis in proliferating but not in post-mitotic cells. *Cell Cycle* 2010; **9**: 97–103.
27. Korenjak M, Anderssen E, Ramaswamy S, Whetstone JR, Dyson NJ. RBF binding to both canonical E2F targets and noncanonical targets depends on functional dE2F/dDP complexes. *Mol Cell Biol* 2012; **32**: 4375–4387.
28. Korenjak M, Taylor-Harding B, Binne UK, Satterlee JS, Stevaux O, Aasland R *et al*. Native E2F/RBF complexes contain Myb-interacting proteins and repress transcription of developmentally controlled E2F target genes. *Cell* 2004; **119**: 181–193.
29. Taylor-Harding B, Binne UK, Korenjak M, Brehm A, Dyson NJ. p55, the Drosophila ortholog of RbAp46/RbAp48, is required for the repression of dE2F2/RBF-regulated genes. *Mol Cell Biol* 2004; **24**: 9124–9136.
30. Lewis PW, Beall EL, Fleischer TC, Georgette D, Link AJ, Botchan MR. Identification of a Drosophila Myb-E2F2/RBF transcriptional repressor complex. *Genes Dev* 2004; **18**: 2929–2940.
31. Lee H, Ohno K, Voskobonyk Y, Ragusano L, Martinez A, Dimova DK. Drosophila RB proteins repress differentiation-specific genes via two different mechanisms. *Mol Cell Biol* 2010; **30**: 2563–2577.
32. Georgette D, Ahn S, MacAlpine DM, Cheung E, Lewis PW, Beall EL *et al*. Genomic profiling and expression studies reveal both positive and negative activities for the Drosophila Myb MuvB/dREAM complex in proliferating cells. *Genes Dev* 2007; **21**: 2880–2896.
33. Acharya P, Negre N, Johnston J, Wei Y, White KP, Henry RW *et al*. Evidence for autoregulation and cell signaling pathway regulation from genome-wide binding of the Drosophila retinoblastoma protein. *G3 (Bethesda)* 2012; **2**: 1459–1472.
34. Frolov MV, Moon NS, Dyson NJ. dDP is needed for normal cell proliferation. *Mol Cell Biol* 2005; **25**: 3027–3039.
35. Bosco G, Du W, Orr-Weaver TL. DNA replication control through interaction of E2F-RB and the origin recognition complex. *Nat Cell Biol* 2001; **3**: 289–295.
36. Reuveny A, Elhanany H, Volk T. Enhanced sensitivity of midline glial cells to apoptosis is achieved by HOW(L)-dependent repression of Diap1. *Mech Dev* 2009; **126**: 30–41.
37. Volk T, Israeli D, Nir R, Toledano-Katchalski H. Tissue development and RNA control: 'HOW' is it coordinated? *Trends Genet* 2008; **24**: 94–101.
38. Marchal C, Vinatier G, Sanial M, Plessis A, Pret AM, Limbourg-Bouchon B *et al*. The HIV-1 Vpu protein induces apoptosis in Drosophila via activation of JNK signaling. *PLoS One* 2012; **7**: e34310.
39. Acharya P, Raj N, Buckley MS, Zhang L, Duperon S, Williams G *et al*. Paradoxical instability-activity relationship defines a novel regulatory pathway for retinoblastoma proteins. *Mol Biol Cell* 2010; **21**: 3890–3901.
40. Tower J. Developmental gene amplification and origin regulation. *Annu Rev Genet* 2004; **38**: 273–304.
41. Wichmann A, Uyetake L, Su TT. E2F1 and E2F2 have opposite effects on radiation-induced p53-independent apoptosis in Drosophila. *Dev Biol* 2010; **346**: 80–89.
42. Rovani MK, Brachmann CB, Ramsay G, Katzen AL. The dREAM/Myb-MuvB complex and Grim are key regulators of the programmed death of neural precursor cells at the Drosophila posterior wing margin. *Dev Biol* 2012; **372**: 88–102.
43. Moon NS, Frolov MV, Kwon EJ, Di Stefano L, Dimova DK, Morris EJ *et al*. Drosophila E2F1 has context-specific pro- and antiapoptotic properties during development. *Dev Cell* 2005; **9**: 463–475.
44. Quinn L, Coombe M, Mills K, Daish T, Colussi P, Kumar S *et al*. Buffy, a Drosophila Bcl-2 protein, has anti-apoptotic and cell cycle inhibitory functions. *EMBO J* 2003; **22**: 3568–3579.
45. Sevrioukov EA, Burr J, Huang EW, Assi HH, Monserrate JP, Purves DC *et al*. Drosophila Bcl-2 proteins participate in stress-induced apoptosis, but are not required for normal development. *Genesis* 2007; **45**: 184–193.
46. Berge EO, Knappskog S, Geisler S, Staalesen V, Pacal M, Borresen-Dale AL *et al*. Identification and characterization of retinoblastoma gene mutations disturbing apoptosis in human breast cancers. *Mol Cancer* 2010; **9**: 173.
47. Sharma A, Comstock CE, Knudsen ES, Cao KH, Hess-Wilson JK, Morey LM *et al*. Retinoblastoma tumor suppressor status is a critical determinant of therapeutic response in prostate cancer cells. *Cancer Res* 2007; **67**: 6192–6203.
48. Bertin-Ciftci J, Barre B, Le Pen J, Maillet L, Cournaud C, Juin P *et al*. pRb/E2F-1-mediated caspase-dependent induction of Noxa amplifies the apoptotic effects of the Bcl-2/Bcl-xL inhibitor ABT-737. *Cell Death Differ* 2013; **20**: 755–764.
49. Yin D, Ogawa S, Kawamata N, Tunico P, Finocchiaro G, Eoli M *et al*. High-resolution genomic copy number profiling of glioblastoma multiforme by single nucleotide polymorphism DNA microarray. *Mol Cancer Res* 2009; **7**: 665–677.
50. Bian Y, Wang L, Lu H, Yang G, Zhang Z, Fu H *et al*. Downregulation of tumor suppressor QKI in gastric cancer and its implication in cancer prognosis. *Biochem Biophys Res Commun* 2012; **422**: 187–193.
51. Zhao Y, Zhang G, Wei M, Lu X, Fu H, Feng F *et al*. The tumor suppressing effects of QKI-5 in prostate cancer: a novel diagnostic and prognostic protein. *Cancer Biol Ther* 2014; **15**: 108–118.
52. Zhao Y, Tan J, Zhuang L, Jiang X, Liu ET, Yu Q. Inhibitors of histone deacetylases target the Rb-E2F1 pathway for apoptosis induction through activation of proapoptotic protein Bim. *Proc Natl Acad Sci USA* 2005; **102**: 16090–16095.
53. Hao H, Dong Y, Bowling MT, Gomez-Gutierrez JG, Zhou HS, McMasters KM. E2F-1 induces melanoma cell apoptosis via PUMA up-regulation and Bax translocation. *BMC Cancer* 2007; **7**: 24.
54. Brun S, Rincheval V, Gaumer S, Mignotte B, Guenal I. reaper and bax initiate two different apoptotic pathways affecting mitochondria and antagonized by bcl-2 in Drosophila. *Oncogene* 2002; **21**: 6458–6470.
55. Coleno-Costes A, Jang SM, de Vanssay A, Rougeot J, Bouceba T, Randsholt NB *et al*. New partners in regulation of gene expression: the enhancer of Trithorax and Polycomb Corto interacts with methylated ribosomal protein l12 via its chromodomain. *PLoS Genet* 2012; **8**: e1003006.



**Cell Death and Disease is an open-access journal published by Nature Publishing Group. This work is**

**licensed under a Creative Commons Attribution-NonCommercial-ShareAlike 3.0 Unported License. The images or other third party material in this article are included in the article's Creative Commons license, unless indicated otherwise in the credit line; if the material is not included under the Creative Commons license, users will need to obtain permission from the license holder to reproduce the material. To view a copy of this license, visit <http://creativecommons.org/licenses/by-nc-sa/3.0/>**

Supplementary Information accompanies this paper on Cell Death and Disease website (<http://www.nature.com/cddis>)